Journal of Electronic Research and Application, 2026, Volume 10, Issue 6
http://ojs.bbwpublisher.com/index.php/JERA
Online ISSN: 2208-3510
Print ISSN: 2208-3502

Structure- and Frequency-aware Domain Adaptation for SAR Raft Aquaculture Extraction

Yijie Wu, Shan Jiang*

School of Information Science and Engineering, Dalian Polytechnic University, Dalian 116034, China

Author to whom correspondence should be addressed.

Abstract: Marine aquaculture is an important part of the marine economy in China. Synthetic aperture radar (SAR) images can work at all times, which makes them suitable for large-scale monitoring of aquaculture areas. However, SAR images from different regions often have obvious differences in background scattering, aquaculture structures, and imaging conditions. These differences cause serious domain shift problems and reduce the segmentation performance of existing methods in cross-region tasks. To solve this problem, this paper proposes a structure- and frequency-aware domain adaptation method (SFDA) for raft aquaculture extraction from SAR images. The method includes a directional structure alignment (DSA) module and a frequency domain alignment (FDA) module. The DSA module aligns the directional structure features between the source and target domains, while the FDA module aligns texture and scattering features in the frequency domain. Experiments on the Gaofen-3 SAR dataset from Jiangsu province show that the proposed method is effective for cross-region raft aquaculture extraction.

Keywords: Transfer learning; Unsupervised domain adaptation; SAR; Marine aquaculture

Online publication: Jul 23, 2026

1. Introduction

In recent years, the offshore raft aquaculture industry has become an important component of the coastal economy and has developed rapidly in China [1]. Accurate extraction of raft aquaculture areas is of great practical significance for marine resource management, marine environmental monitoring, and sustainable aquaculture planning. Synthetic aperture radar (SAR) imagery is less affected by weather and illumination conditions, enabling all-time observation of offshore aquaculture areas. Therefore, SAR remote sensing technology has been widely applied in the extraction of raft aquaculture areas [2].

Traditional raft aquaculture extraction methods mainly rely on manually designed features and threshold-based segmentation strategies. Although these methods can achieve satisfactory results in simple scenes, they generally suffer from poor robustness in complex marine environments. With the rapid development of deep learning techniques, convolutional neural network-based semantic segmentation algorithms have significantly improved the extraction accuracy of marine aquaculture targets and demonstrated excellent performance [3]. Wang et al. proposed the MDOAU-net model, which integrates multi-scale feature fusion, atrous convolution, and deformable convolution into the attention U-Net architecture for SAR image aquaculture area segmentation [4]. Fan et al. proposed a method based on complex-valued convolutional neural networks for SAR aquaculture recognition. The method uses phase information in polarimetric SAR data and improves detection results on Gaofen-3 (GF-3) images [5]. Wang et al. proposed the IDUDL model for marine aquaculture extraction in SAR images [6]. The model updates pseudo labels step by step to support semantic extraction and incremental learning. However, SAR images from different sea areas often have large distribution differences. These methods work well in one region, but their performance usually decreases when applied to other regions. This makes cross-region generalization difficult.

Unsupervised domain adaptation (UDA) is widely used to reduce differences between domains. It transfers knowledge from a labeled source domain to an unlabeled target domain. Common methods include feature alignment, style transfer, and pseudo-label generation [7–9]. UDA achieved remarkable performance in urban scene segmentation and is widely applied in SAR tasks, such as vehicle classification, ship detection, land cover classification, and oil spill segmentation [10–16]. These studies show that UDA can improve cross-domain performance. However, raft aquaculture extraction in SAR images is still difficult.

SAR images from different coastal regions often show large differences because of sea conditions, imaging geometry, incidence angles, and speckle noise. These differences lead to large domain gaps between the source domain and the target domain. Raft aquaculture areas also have regular strip-like shapes and obvious directional features. Most existing domain adaptation methods focus on semantic features and ignore structural information. Because of this, the extracted features from different domains often do not keep good structural consistency. At the same time, SAR images differ not only in texture information but also in spectral distributions, which further increases the difficulty of cross-region adaptation.

To reduce the domain gap in cross-region SAR raft aquaculture extraction, this paper develops a structure- and frequency-aware domain adaptation framework based on ADVENT [17]. The framework contains two adaptation modules. One is the directional structure alignment (DSA) module. It aligns directional features from the source and target domains, helping the model preserve similar structural patterns across domains. The other is the frequency domain alignment (FDA) module. This module reduces spectral differences in SAR images by aligning low-frequency components in the Fourier domain.

2. Proposed method

2.1. Overview

The overall framework of SFDA is shown in **Figure 1**. The framework uses ADVENT as the basic domain adaptation model and further applies alignment in both spatial and frequency domains to reduce differences between SAR scenes.

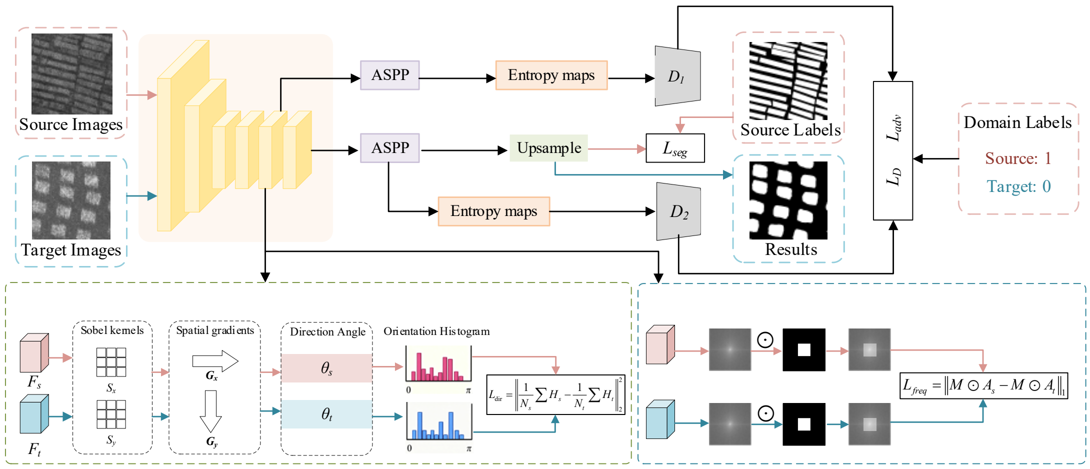

Figure 1. Architecture of the proposed structure- and frequency-aware domain adaptation framework.

2.2. ADVENT-based domain adaptation framework

Let the labeled source domain and the unlabeled target domain be denoted as $\mathcal{D}_s = \{(x_s, y_s)\}$ and $\mathcal{D}_t = \{x_t\}$, respectively. The segmentation network G predicts the probability map $P = G(x)$. For source-domain samples, standard supervised segmentation loss is employed:

$$L_{\text{seg}} = -\sum_{h,w}\sum_{c=1}^{C} y_s^{(h,w,c)} \log P_s^{(h,w,c)} \tag{1}$$

where C denotes the number of classes, and $P_s^{(h,w,c)}$ represents the predicted probability that the source-domain pixel belongs to class c. Following ADVENT, normalized entropy maps are constructed as

$$E(x) = -\frac{1}{\log C}\sum_{c=1}^{C} P^{(c)} \log P^{(c)} \tag{2}$$

The entropy map reflects the prediction uncertainty, where source-domain predictions usually exhibit lower entropy values, while target-domain predictions tend to have higher entropy values. Subsequently, the entropy maps of the source and target domains are fed into the domain discriminator D for adversarial learning. The domain discriminator, which aims to distinguish source-domain predictions from target-domain predictions, while the segmentation network attempts to confuse the discriminator. The discriminator loss is

$$L_D = -\mathbb{E}_{x_s}\left[\log D(E_s)\right] - \mathbb{E}_{x_t}\left[\log\left(1 - D(E_t)\right)\right] \tag{3}$$

The adversarial objective for the segmentation network is

$$L_{\text{adv}} = -\mathbb{E}_{x_t}\left[\log D(E_t)\right] \tag{4}$$

Through entropy adversarial learning, the prediction distribution of the target domain is gradually aligned with that of the source domain.

2.3. Direction structure alignment

Raft aquaculture regions in SAR imagery usually exhibit highly regular directional structures due to an artificial parallel arrangement. Although the appearance characteristics vary significantly across regions, the directional continuity and structural consistency remain relatively stable. Conventional domain adaptation methods mainly focus on semantic feature alignment while ignoring such structural priors. Consequently, the extracted features may still suffer from structural inconsistency under large domain shifts. To address this issue, a direction structure alignment module is designed to align the directional distribution of source and target features explicitly.

Let $F_s \in \mathbb{R}^{C\times H\times W}$ and $F_t \in \mathbb{R}^{C\times H\times W}$ denote the intermediate features extracted by the encoder from the source and target domains, respectively. Spatial gradients are first computed using Sobel operators.

$$\begin{aligned} G_x &= F * S_x \\ G_y &= F * S_y \end{aligned} \tag{5}$$

where S_x and S_y denote horizontal and vertical Sobel kernels, respectively, and $*$ denotes the convolution operation. The local directional angle is then calculated as

$$\theta = \arctan\left(\frac{G_y}{G_x + \epsilon}\right) \tag{6}$$

where, ϵ epsilonϵ is a small constant to avoid numerical instability. To characterize the global directional distribution, orientation histograms are constructed over the feature maps:

$$H(\theta) = \text{Histogram}(\theta) \tag{7}$$

The histogram bins represent different orientation intervals within $[0,\pi]$.

To reduce directional discrepancy across domains, the orientation distributions of source and target domains are aligned using Maximum Mean Discrepancy (MMD) [18]:

$$L_{\text{dir}} = \left\| \frac{1}{N_s}\sum H_s - \frac{1}{N_t}\sum H_t \right\|_2^2 \tag{8}$$

where, H_s and H_t denote orientation histograms of source and target domains, N_s and N_t represent the number of samples.

Through direction structure alignment, the network can learn more stable cross-domain structural features, thereby improving the generalization capability under complex marine conditions.

2.4. Frequency domain alignment

In SAR imagery, domain discrepancy is not only reflected in spatial appearance but also in spectral characteristics caused by imaging conditions, sea states, and speckle noise. Low-frequency components mainly encode global imaging style and illumination statistics, while high-frequency components preserve structural details of raft targets. Therefore, aligning low-frequency spectral information can effectively reduce style discrepancy between domains while maintaining target structures.

For a feature map F, the 2D Fourier transform is computed as:

$$\mathcal{F}(u,v) = \sum_{x=0}^{H-1}\sum_{y=0}^{W-1} F(x,y)e^{-j2\pi(ux/H+vy/W)} \tag{9}$$

The Fourier representation can be decomposed into amplitude and phase components:

$$\mathcal{F}(u,v) = A(u,v)e^{j\phi(u,v)} \tag{10}$$

where, $A(u,v)$ denotes the amplitude spectrum, $\phi(u,v)$ denotes the phase spectrum. Since low-frequency components dominate domain-specific imaging styles, only the central low-frequency region is aligned. A low-frequency mask M is defined as

$$M(u,v)=\begin{cases}1, & (u,v)\in\Omega \\ 0, & \text{otherwise}\end{cases} \tag{11}$$

where Ω denotes the low-frequency region. The frequency alignment loss is formulated as

$$L_{freq}=\left\|M\odot A_s-M\odot A_t\right\|_1 \tag{12}$$

where, A_s and A_t denote the amplitude spectra of source and target features, $\odot$ represents element-wise multiplication.

By aligning low-frequency spectral distributions, the proposed module effectively mitigates SAR imaging-style discrepancy across domains.

2.5. Overall optimization

The final training objective is

$$L_{\text{total}}=L_{\text{seg}}+\lambda_{\text{adv}}L_{\text{adv}}+\lambda_{\text{dir}}L_{\text{dir}}+\lambda_{\text{freq}}L_{\text{freq}} \tag{13}$$

where, L_{seg} denotes supervised segmentation loss on the source domain, L_{adv} denotes the adversarial entropy alignment loss in ADVENT, L_{dir} denotes the proposed direction structure alignment loss, L_{freq} denotes the proposed frequency-domain alignment loss.

During training, the optimization process alternately updates the segmentation network to minimize the segmentation and alignment losses, while updating the discriminator to enhance its capability of distinguishing source and target domains.

Through joint spatial-directional and frequency-domain alignment, the proposed framework learns more robust domain-invariant representations for cross-region SAR raft aquaculture extraction.

3. Experiments

3.1. Datasets

Both the source and target domain datasets are constructed using 3 m spatial resolution GF-3 ultra-fine strip map (UFS) mode SAR images. The source domain is collected from Changhai County, Liaoning province, while the target domain is collected from Jiangsu province. All images are cropped into image patches of 512×512 pixels. A total of 1000 image patches are generated for the source domain, whereas 96 image patches are selected for the target domain and divided into training and testing sets at a ratio of 84:12.

3.2. Evaluation metrics

To comprehensively evaluate the segmentation performance of the proposed method on the target domain, five commonly used evaluation metrics were used are adopted in this paper: mean Intersection over Union (*mIoU*), Overall Accuracy (*OA*), Precision (*P*), Recall (*R*), and F1-score (*F1*). Among them, the positive class corresponds to aquaculture areas, while the negative class corresponds to the surrounding seawater regions [19].

3.3. Implementation details

All experiments are conducted in PyTorch 1.9.0 using an Intel Xeon W5-3435X with a clock speed of 3.1GHz and an NVIDIA GeForce RTX 4090. The hyperparameters λ_{adv}, λ_{dir}, and λ_{freq} are empirically set to 0.001, 0.01, and 0.01, respectively.

3.4. Comparison results

To validate the effectiveness of the proposed SFDA method, three representative methods are selected for comparison: K-Means and ADVENT, and RoadDA [17,20]. All comparative experiments are conducted under the same settings. The visualization results of the predictions are shown in Figure 2, while the quantitative metrics are presented in **Table 1**. The proposed method achieves an mIoU of 0.7677 on the target domain, which is 0.0487 higher than that of RoadDA.

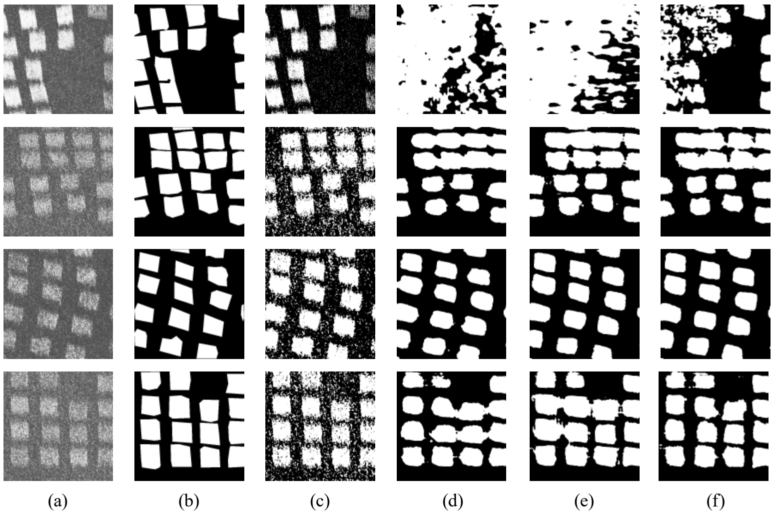

Figure 2. Comparative experimental results of floating raft aquaculture segmentation in Jiangsu province. (a) Original images. (b) Ground truth. (c) K-Means (d) ADVENT. (e) RoadDA. (f) SFDA.

Table 1. Evaluation results on the shared Jiangsu dataset

Methods	***mIoU***	***OA*(%)**	***P*(%)**	***R*(%)**	***F1***
K-Means	0.6719	81.04	68.96	85.30	0.7627
ADVENT [17]	0.7092	83.79	73.86	84.52	0.7883
RoadDA [20]	0.7190	84.30	73.26	88.21	0.8004
SFDA(Ours)	0.7677	87.92	84.56	80.95	0.8272

3.5. Ablation experiment

To further validate the effectiveness of each module, ablation experiments are conducted, and the results are summarized in Tab. II. First, the performance of models equipped with only the DSA module or only the FDA module is evaluated. The corresponding mean mIoU values reach 0.7427 and 0.7513, respectively. When both DSA and FDA are jointly incorporated, the mIoU is further improved to 0.7677. These results demonstrate the effectiveness and complementary characteristics of the proposed modules within the overall framework. See **Table 2.**

Table 2. Results of ablation experiments

DSA	**FDA**	***mIoU*(%)**	***OA*(%)**	***F1***
		0.7092	83.79	0.7883
✓		0.7427	86.19	0.8105
	✓	0.7513	86.92	0.8136
✓	✓	0.7677	87.92	0.8272

4. Conclusion

This paper presents a structure- and frequency-aware domain adaptation framework, SFDA, for cross-region raft aquaculture extraction in SAR images. The framework includes the DSA module and the FDA module to align features between the source and target domains from both the structure and frequency views. This helps reduce the domain gap caused by different regions in SAR data and improves segmentation accuracy and generalization.

Disclosure statement

The authors declare no conflict of interest.

References

[1] Pörtner H O, Scholes R, Arneth A, et al., 2023, Overcoming the Coupled Climate and Biodiversity Crises and Their Societal Impacts. Science, 380(6642): eabl4881.

[2] Fan J, Zhao J, Song D, et al., 2018, Marine Floating Raft Aquaculture Dynamic Monitoring Based on Multi-Source GF Imagery. 2018 7th International Conference on Agro-Geoinformatics, 1–4.

[3] Chen W, Li X, 2024, Deep-Learning-Based Marine Aquaculture Zone Extractions from Dual-Polarimetric SAR Imagery. IEEE Journal of Selected Topics in Applied Earth Observations and Remote Sensing, 17: 8043–8057.

[4] Wang J, Fan J, Wang J, 2022, MDOAU-Net: A Lightweight and Robust Deep Learning Model for SAR Image Segmentation in Aquaculture Raft Monitoring. IEEE Geoscience and Remote Sensing Letters, 19: 1–5.

[5] Fan J, Zhao J, An W, et al., 2019, Marine Floating Raft Aquaculture Detection of GF-3 PolSAR Images Based on Collective Multikernel Fuzzy Clustering. IEEE Journal of Selected Topics in Applied Earth Observations and Remote Sensing, 12(8): 2741–2754.

[6] Wang X, Zhou J, Fan J, 2022, IDUDL: Incremental Double Unsupervised Deep Learning Model for Marine Aquaculture SAR Images Segmentation. IEEE Transactions on Geoscience and Remote Sensing, 60: 1–12.

[7] Zhao J, Li Y, Zhou Y, et al., 2025, DDCI: Unsupervised Domain Adaptation for Remote Sensing Images Based on Diffusion Causal Distillation. IEEE Transactions on Geoscience and Remote Sensing, 63: 1–12.

[8] Zhu J, Guo Y, Sun G, et al., 2024, Causal Prototype Inspired Contrast Adaptation for Unsupervised Domain Adaptive Semantic Segmentation of High-Resolution Remote Sensing Imagery. IEEE Transactions on Geoscience and Remote Sensing, 62: 1–17.

[9] Zhu C, Liu K, Tang W, et al., 2025, Hard-Aware Instance Adaptive Self-Training for Unsupervised Cross-Domain Semantic Segmentation. IEEE Transactions on Pattern Analysis and Machine Intelligence, 47(7): 5655–5671.

[10] Shi Y, Du L, Li C, et al., 2024, Unsupervised Domain Adaptation for SAR Target Classification Based on Domain- and Class-Level Alignment: From Simulated to Real Data. ISPRS Journal of Photogrammetry and Remote Sensing, 207: 1–13.

[11] Yang Y, Chen J, Sun L, et al., 2024, Unsupervised Domain-Adaptive SAR Ship Detection Based on Cross-Domain Feature Interaction and Data Contribution Balance. Remote Sensing, 16(2): 420.

[12] Liu S, Li D, Song H, et al., 2025, SAR Ship Detection Across Different Spaceborne Platforms with Confusion-Corrected Self-Training and Region-Aware Alignment Framework. ISPRS Journal of Photogrammetry and Remote Sensing, 228: 305–322.

[13] Yang Y, Yang X, Yang D, 2025, Unsupervised Domain Adaptation for SAR Ship Detection Based on Multitask

Decoupling. IEEE Journal of Selected Topics in Applied Earth Observations and Remote Sensing, 18: 12684–12696.

[14] Tu H, Wang W, Guo Y, et al., 2025, Mamba-UDA: Mamba Unsupervised Domain Adaptation for SAR Ship Detection. IEEE Geoscience and Remote Sensing Letters, 22: 1–5.

[15] Ren Z, Du Z, Zhang Y, et al., 2024, Multi-Step Unsupervised Domain Adaptation in Image and Feature Space for Synthetic Aperture Radar Image Terrain Classification. Remote Sensing, 16(11): 1901.

[16] Cui G, Fan J, Zou Y, 2025, Enhanced Unsupervised Domain Adaptation with Iterative Pseudo-Label Refinement for Inter-Event Oil Spill Segmentation in SAR Images. International Journal of Applied Earth Observation and Geoinformation, 139: 104479.

[17] Vu T, Jain H, Bucher M, et al., 2019, ADVENT: Adversarial Entropy Minimization for Domain Adaptation in Semantic Segmentation. Proceedings of the IEEE/CVF Conference on Computer Vision and Pattern Recognition (CVPR), 2512–2521.

[18] Arthur G, Karsten M B, Malte J R, et al., 2012, A Kernel Two-Sample Test. Journal of Machine Learning Research, 13(25): 723–773.

[19] Fan J, Li M, Wang X, 2025, Unsupervised Transformer with Generative Label Optimization for Marine Aquaculture Segmentation. IEEE Transactions on Geoscience and Remote Sensing, 63: 1–14.

[20] Zhang L, Lan M, Zhang J, et al., 2022, Stagewise Unsupervised Domain Adaptation with Adversarial Self-Training for Road Segmentation of Remote-Sensing Images. IEEE Transactions on Geoscience and Remote Sensing, 60: 1–13.